Progress In Electromagnetics Research C, Vol. 57, 71–79, 2015

Design and Simulation of a Single Fed Multi-Band Circularly Polarized Microstrip Antenna with Slots

Mai F. Ahmed[1, *], Abdel H. Shaalan[1], and Kamal H. Awadalla[2]

Abstract—Nowadays the mobile personal communication systems and wireless networks are commonly used. Experience has revealed that the antennas suitable for these applications should have small size and operate in assigned different frequency bands. For this purpose, circularly polarized (CP) multi-band square microstrip antenna with three N-slots and a pair of truncated corners is proposed, designed and simulated. To reduce the losses and improve the antenna efficiency in addition to the bandwidth, an efficient electromagnetic band gap (EBG) structure is introduced. The proposed antenna has produced a higher efficiency, an improved operational bandwidth, and a higher gain relative to the conventional microstrip antenna.

1. INTRODUCTION

A circularly polarized (CP) microstrip antenna is an excellent candidate for portable wireless devices. Personal mobile communications requires small size and light weight antenna with wideband performance. Circular polarization is beneficial because current and future applications require the additional design freedom of no alignment of the electric field vector at receiving and transmitting locations. Single feed circularly polarized antennas are currently receiving much attention because the single feed allows a reduction in the complexity, weight and RF losses of any array feed and is desirable in situations where it is difficult to accommodate dual orthogonal feeds with a power divider network [1].

When the feed location is on one of the orthogonal axes (X or Y) of the patch radiator, any arbitrarily shaped cuts such as truncated corners along the diagonal directions acts as a perturbation of the microstrip patch to excite two orthogonal modes with a 90° phase shift for the circularly polarized radiation requirements [2]. The perturbation cut should be close to 45° relative to the feed location axis. Truncated corners along anyone of the diagonal directions of the patch can realize such condition [2]. By slightly changing the size of the truncated corners in the diagonal directions and fix their orientation at 45° relative to the axes of a rectangular parch, two orthogonal resonant modes can be achieved and therefore produce the circularly polarized radiation requirements [2]. The two orthogonal modes should have close magnitudes to realize circular polarization. This can be achieved by positioning the feed on an axis of symmetry of the radiating patch and close to the diagonal joining the cut corners. This in fact is agreeing with the characteristic modes explained in [3].

As such, many researchers are focusing on the development of patch antenna for performance enhancement. This has been relatively achieved using different slot shapes inserted in the patch [4–10]. However, they have realized single frequency circular radiation characteristics.

In this paper, a circularly polarized N-shaped slotted microstrip patch antenna that is significantly smaller than the conventional patch antenna is presented and has realized multi-band circular radiation characteristics.

Received 4 February 2015, Accepted 9 April 2015, Scheduled 27 April 2015

* Corresponding author: Mai Fouad Ahmed (mfabdelhalim@zu.edu.eg).

[1] Department of Electrical & Electronics Engineering, Faculty of Engineering, Zagazig University, Zagazig, Egypt. [2] Department of Electronics and Communication Engineering, Faculty of Electronic Engineering, Menoufiya University, Menoufiya, Egypt.

A single-feed circularly polarized microstrip antenna configuration has been achieved at a relatively low gain, narrow impedance bandwidth and multi narrow band circularly polarized radiation. Therefore, another design with an electromagnetic band gap (EBG) structure is proposed and included to improve these parameters.

With EBGs, forbidden frequency bands pertain to EM waves that are scattered within the structure and destructively added. Hence, EM waves with a frequency inside the forbidden band cannot propagate through the EBG material, irrespective of their angle of incidence [11]. EBGs could be as well used to improve the efficiency of antennas [12], due to the suppression of surface waves and substrate losses, which are the predominant loss mechanisms in microstrip antennas.

2D-EBGs are of particular interest at microwave frequencies, due to ease of fabrication and suitability to microstrip patch antennas. These EBGs are usually only periodic in a 2D plane and do not exhibit a band gap for all angles of incidence of an EM wave, but just for all angles in that one plane.

There are various numerical methods to analyse the EBG structures [13]. However, to determine the forbidden frequency bands of such structures, one has to construct the dispersion diagram for it. The plane wave expansion method (PWM) [14] is used in the analysis of electromagnetic band gap structures to construct the dispersion diagram. The band gap is found to correspond to the frequency band within which any propagating modes are not allowed. PWM is an analytical method based on the expansion of the (E or H) field with discrete Fourier series expressed on the plane wave basis. Such Fourier expansion is possible when the medium is supposed to be periodic. The full wave analysis can then be obtained by implementing the expansion terms in Maxwell's equations [15].

For the periodic structure, the maximum band gap occurs when the radius of the air holes was $r_{\max} = 0.48a$, where "a" is the in-plane lattice constant [16]. The lattice constant of the material "a" refers to the repetition distance (or periodicity) in the horizontal plan [17]. The periodicity in relation to the guided wavelength λ_g is of a different order of magnitude. The period p for EBGs is of the order of half a guided wavelength: $p \sim \lambda_g/2$ [18]. The guided wavelength is given by $\lambda_g = v/f_s$, where v is the velocity of the electromagnetic wave within the substrate and is equal to $c/(\varepsilon_{re})^{0.5}$, ε_{re} is the effective dielectric constant and f_s is the wave frequency [19]. Accordingly, the radius and periodicity of the holes for the desired bandwidth have been optimized such that, the radius $r = 2\,\text{mm}$ and the periodicity $p = 7\,\text{mm}$ to improve the antenna performance with a relaxed manufacturing tolerance.

The EBG structure has been selected to be a triangular lattice. The Brillouin zone in triangular lattice is formed as a hexagonal shape. The band gap is computed for TE polarization and the dispersion curves are shown in Figure 1.

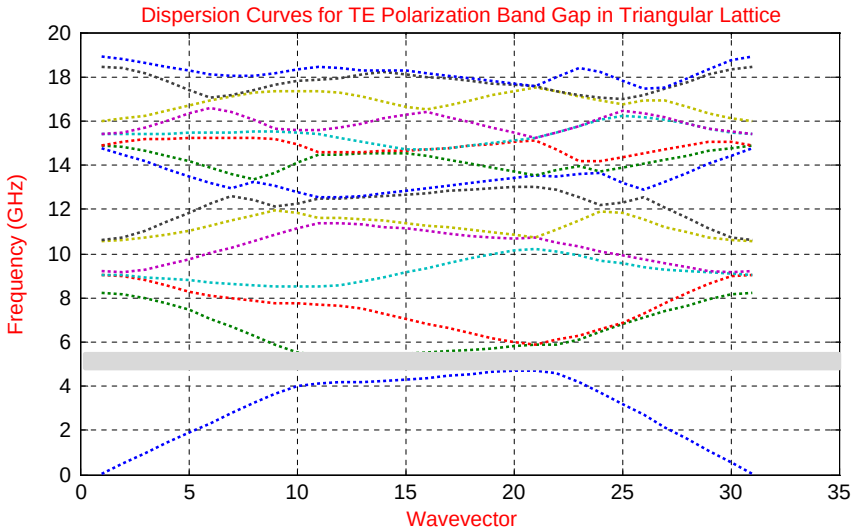

Figure 1. The dispersion diagram of triangular lattice for TE polarization.

2. ANTENNA GEOMETRY

Figure 2 illustrates the geometry of the basic microstrip antenna. This antenna is the same as that given in [20]. Figure 3(b) depicts the multi-band circularly polarized microstrip antenna. A square patch with length $L = 28\,\text{mm}$ and the dimensions of the ground plane are $36\,\text{mm} \times 36\,\text{mm}$. The patch antenna and the ground plane are etched on the opposite sides of the substrate which is made from FR4 with thickness $h = 1.6\,\text{mm}$, relative permittivity $\varepsilon_r = 4.2$ and $\tan(\delta) = 0.02$. The square patch is truncated at 45° at two opposite corners on the same diagonal. The antenna is fed with a coaxial probe located at a point at a distance "A" from the patch center on the x-axis to obtain right hand circular polarization (RHCP).

Microstrip patch antennas are usually designed to operate at a feed matching condition. Edge fields are also important and they bring an equivalent additional length to the antenna. This length depends on the relative permittivity of the dielectric, substrate thickness and patch width. One of the most used formulas is given in [21] and they are used to determine the dimensions of this antenna.

Various microstrip patches are shown in Figures 3(a)–3(c) for multi-band CP radiation. All proposed microstrip patch antennas are optimized for good CP radiation. Figure 3(a) shows the conventional truncated corners circular polarized microstrip antenna for comparison. A pair of truncated

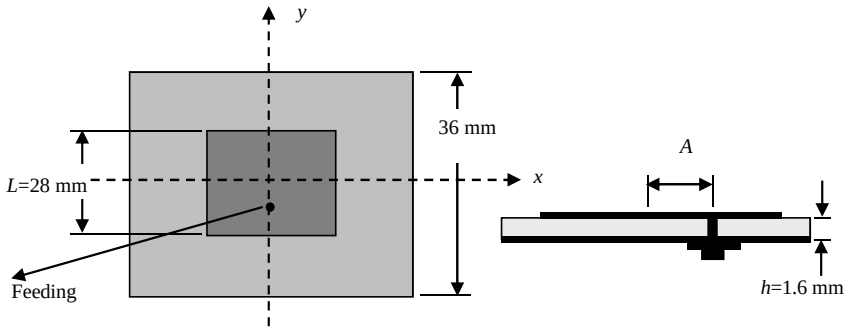

Figure 2. The antenna geometry.

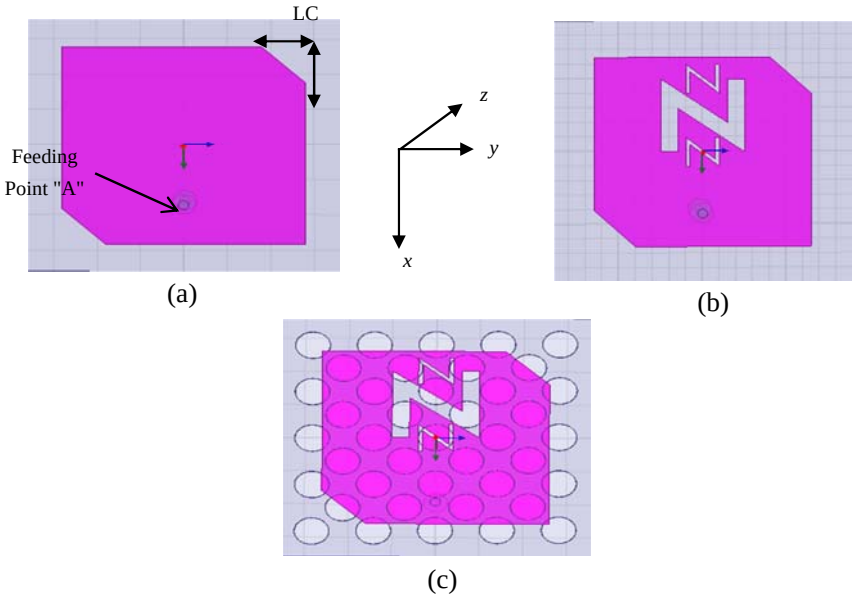

Figure 3. (a) The conventional truncated corners CP microstrip antenna. (b) The truncated corners CP microstrip antenna with three N-slots. (c) The truncated corners CP microstrip antenna with three N-slots and the EBG structure with hole radius $r = 2\,\text{mm}$ and periodicity $P = 7\,\text{mm}$.

	W_s	L_s	(X_N, Y_N)
N-slot 1	2	10	$(-5, 0)$
N-slot 2	0.5	4	$(0, 0)$
N-slot 3	0.5	4	$(-10, 0)$

Table 1. Dimensions and positions of N-slot (unit: mm).

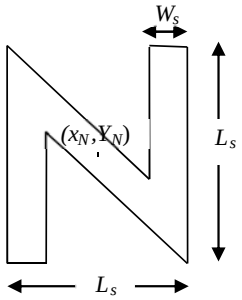

Figure 4. Trade-off curves for Case 1.

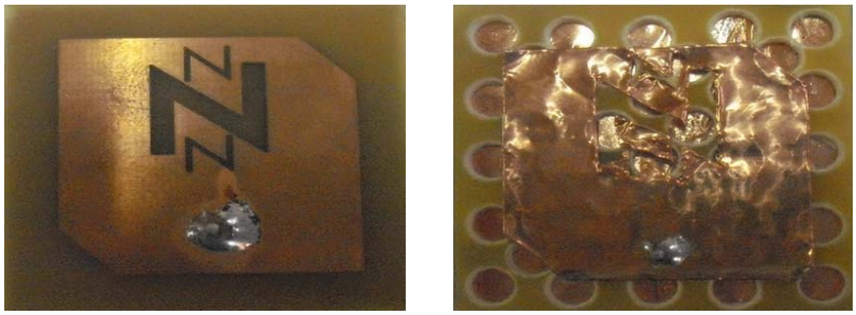

(a) (b)

Figure 5. The fabricated antenna. (a) The truncated corners CP microstrip antenna with three N-slots. (b) The same truncated corners antenna but with EBG in the whole area under the patch.

corners is of equal side length $L_c = 5\,\text{mm}$ and the single probe feed is placed at point $A = 8.5\,\text{mm}$ along the x-axis, a good CP operation is obtained.

The truncated corners circular polarized microstrip antenna with three N-slots for multi-band CP radiation is also designed as illustrated in Figure 3(b). It has to be noted that the N-shaped slot is simple and occupy a smaller area on the patch for the same slot length. This allows multi-slot on the patch to get several frequency bands. Other shaped slots either not as simple or will occupy larger area which restrict the installation of multi-slots. Again, the truncated length $L_c = 5\,\text{mm}$ and the single probe feed is placed at point $A = 9.5\,\text{mm}$ along the x-axis, again a good CP operation is obtained. The dimensions of the N-slots are tuned to broaden the impedance matching bandwidth of the antenna on thick substrate. The best dimensions and positions are tabulated in Table 1 according to Figure 4 with (X_N, Y_N) are the coordinates of the center of the slot.

The patch antenna illustrated in Figure 3(b) with electromagnetic band gap (EBG) structure added in all the area of the substrate is depicted in Figure 3(c). The single probe feed is placed at point $A = 9.6\,\text{mm}$ away from the center on the Y-axis as a result of optimization of the new structure to get good circular polarized performance. The fabricated antenna is shown in Figures 5(a) & (b).

3. RESULTS AND DISCUSSION

The simulated results for the performance of the antennas are tabulated in Table 2. The simulation analysis of these antennas is carried out by applying two commercial software packages. These are HFSS$^{\text{TM}}$ (high frequency selective simulator) [22] from Ansoft and CST STUDIO SUITE$^{\text{TM}}$ 2010 (computer simulation technology antenna simulator) [23]. The two software packages are basically different. The first package is based on the finite element method, but the second package is based on the finite integration technique. Therefore the second has been used to confirm the results determined using the first. Also, experimental measurements for the reflection coefficient S_{11} in only the last two

cases has been carried out and compared with the simulation.

The simulation of reflection coefficient and axial ratio of the conventional truncated corners circularly polarized microstrip antenna (shown in Figure 3(a)) are illustrated in Figures 6(a), 6(b). The figures indicate one resonance at 2.56 GHz with axial ratio of 0 dB at the same frequency and a second resonance at twice the first one, i.e., 5 GHz. The truncated corners have produced a circularly polarized radiation as indicated but only at the first band as expected which is the main resonance band, but the axial ratio is too bad at the second resonance. This is because the current distributions

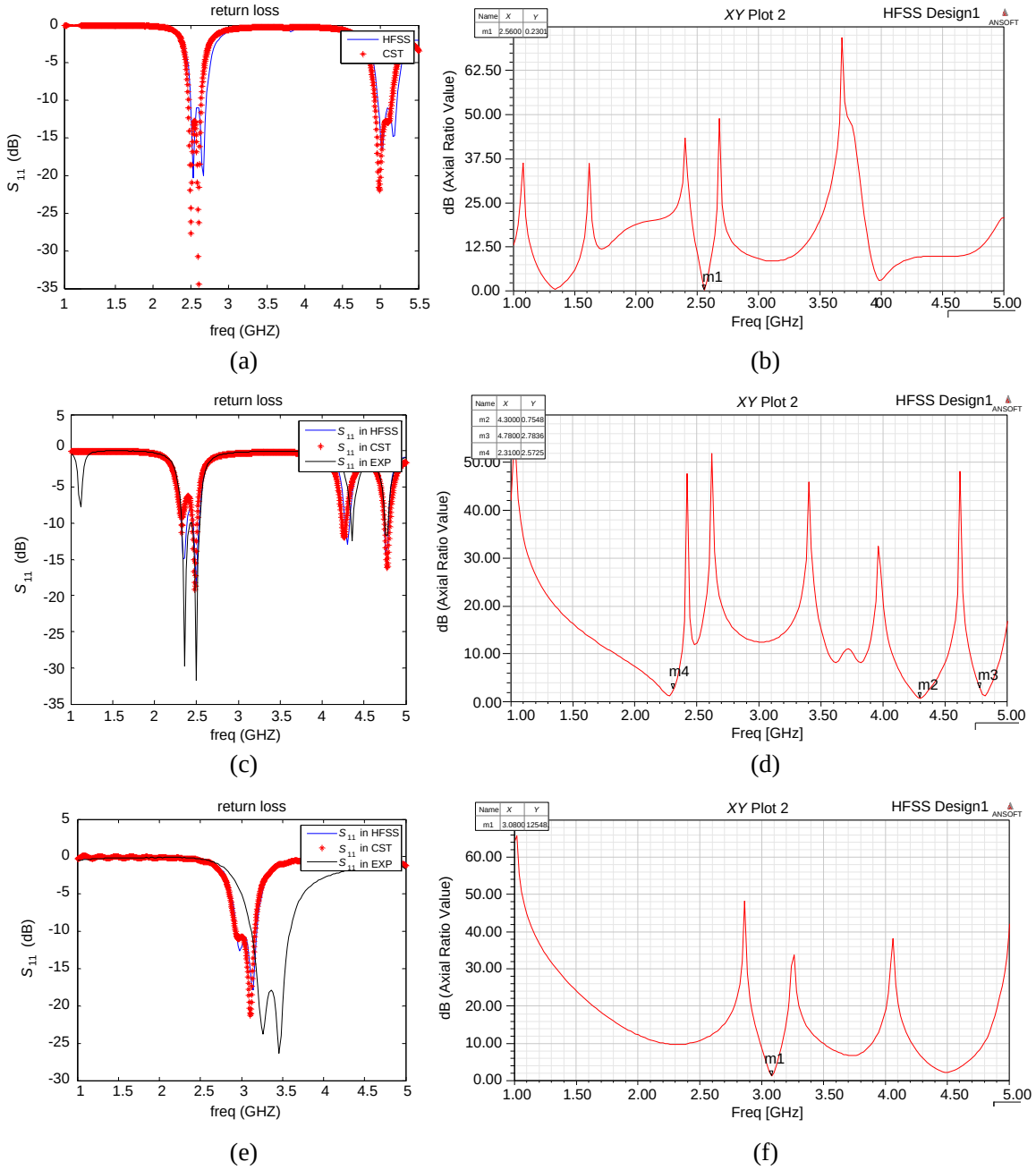

Figure 6. (a) Reflection coefficient against frequency. (b) Axial ratio against frequency. (c) Reflection coefficient against frequency. (d) Axial ratio against frequency. (e) Reflection coefficient against frequency. (f) Axial ratio against frequency.

in the two modes are different.

The simulation results for the reflection coefficient and axial ratio of the truncated corners circular polarized microstrip antenna with three N-slots inserted axially with the feed (as shown in Figure 3(b)) for achieving the multi-band mode are illustrated in Figures 6(c) and 6(d). A comparison with the experimental is given in Figure 6(c) which indicates good agreement of the values of S_{11}. It is the N-slots which actually produced the given multi-bands. The existence of the three N-shaped slots has actually lowered the fundamental resonance frequency that appeared in Figure 6(a) and the 2nd resonance as well which was at the 5 GHz in Figure 6(a). Both resonances have gone down slightly to 2.32 GHz and 4.78 GHz because of the longer current paths on the patch because of the slots as shown in Figure 7. This fact of using slots to enforce longer current paths has been useful to design small microstrip antennas [23–27]. In addition, due to the different sizes of the slots the two resonances are away from each other. However, due to the coupling between the two smaller slots, a third resonance appeared at 4.3 GHz. If one of the two smaller slots disappears, one of the two higher resonances disappears too. The frequency ranges are given in Table 2. Also, one notes that in the experimental results there is a fourth resonance appeared at 1.3 GHz but it did not appear in the two simulated curves. Thus, as it is not pronounced and is lower than the fundamental resonance of the patch, it becomes clear that this resonance came due to the termination of the feeder, which is relatively bulky.

The simulation results of the reflection coefficient and the axial ratio of the same previous antenna but with EBG added in the whole substrate (shown in Figure 3(c)) are illustrated in Figures 6(e)

Table 2. The simulation performance of the multi-band circularly polarized microstrip antenna.

Configuration	3-dB ARBW (GHZ)	ARBW %	Efficiency %	Application
conventional truncated corners CPMA	2.54–2.58	1.56%	20%	WIMAX application
Truncated corners CPMA with N-shaped slots	2.304–2.325	0.918%	17.5%	WIMAX application
	4.273–4.33	1.356%	48.6%	C-band application
	4.767–4.797	0.617%	27%	
Truncated corners CPMA with N-shaped slots and also EBG in the whole substrate under the patch	3.04–3.112	2.179%	62.78%	WIMAX application

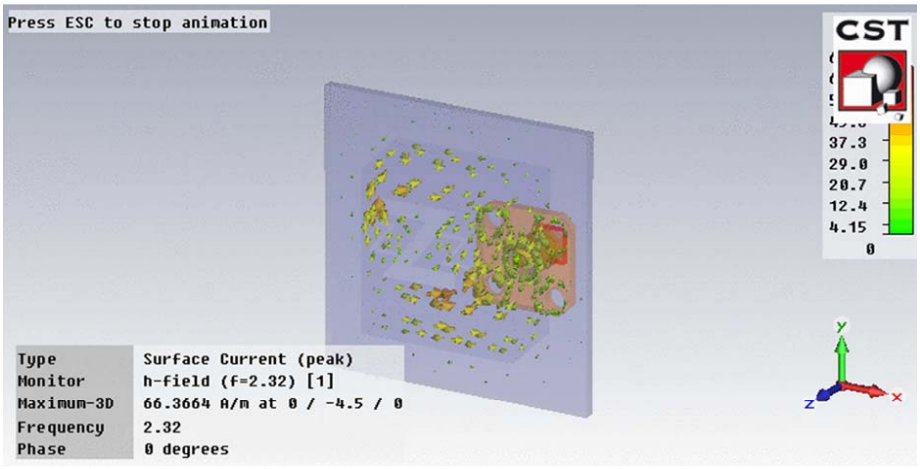

Figure 7. The current distribution of the truncated corners CP microstrip antenna with three N-slots.

and 6(f). The experimental matching frequency band as in the S_{11} curves has shifted up relative to the simulated one by about 0.4 GHz. Obviously, the experimental model has come up with wider tolerance than expected which caused this large shift. The results have revealed an increase in the bandwidth, the gain and the efficiency. That improvement can be attributed to the smaller effective dielectric constant of the substrate with the inserted air holes. Also, it has been noticed that the number of resonant frequencies are less than the previous case with only some of them have realized the CP operation due

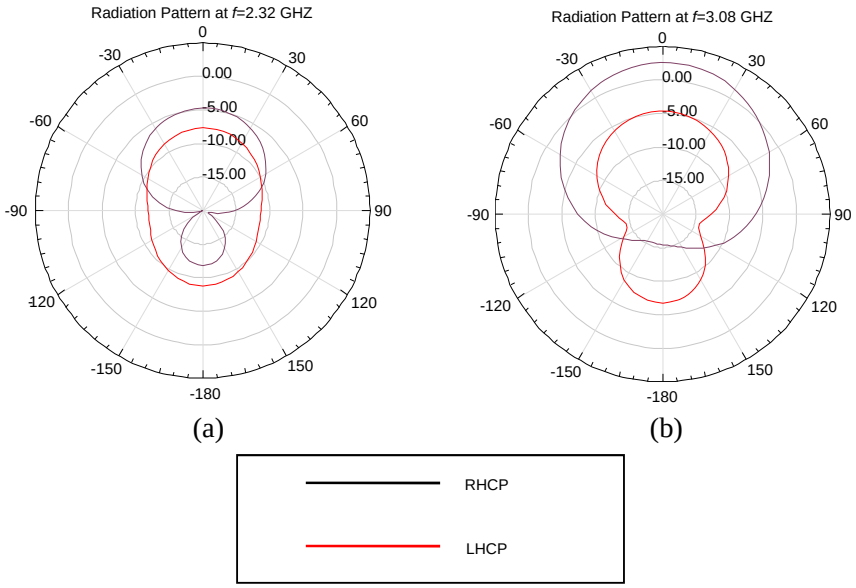

Figure 8. The simulated radiation pattern at $\varphi = 0°$ xz-plane. (a) The truncated corners CP microstrip antenna with three N-slots. (b) The same truncated corners antenna but with EBG in the whole area under the patch.

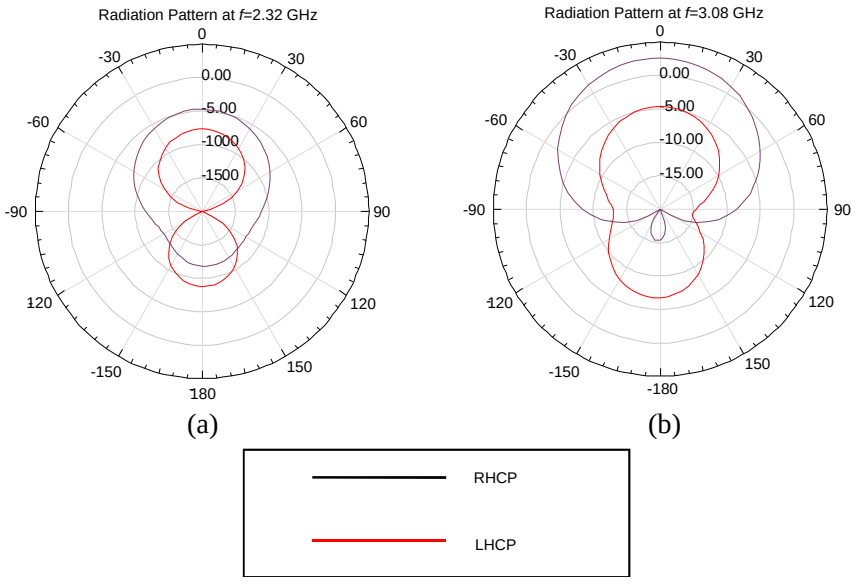

Figure 9. The simulated radiation pattern at $\varphi = 90°$ yz-plane. (a) The truncated corners CP microstrip antenna with three N-slots. (b) The same truncated corners antenna but with EBG in the whole area under the patch.

to the stop band filter used (the EBG structure). The dispersion diagram of triangular lattice for TE polarization is shown in (Figure 1) which confirm the complete band gap occurred between 4.57 GHz and 5.42 GHz. Therefore, the upper two CP bands have vanished because they are too close to the forbidden gap. Also, it has been noticed that the resonant frequencies are shifting up due to decreasing the effective dielectric constant ε_r. This, of course, has shifted up the two higher CP bands and makes them coincide with the forbidden gap. However, the performance has improved because of the efficiency improvement, which has taken place due to the increased number of air holes used that caused a lower effective dielectric constant and lower surface wave and substrate losses. Another effect of lowering the effective ε_r is the shifting up of the fundamental resonance frequency to 3.08 GHz with wider CP bandwidth where the CP band in this case extends from 2.939 GHz to 3.21 GHz. Of course, if one wants to restore the previous main resonance, the size of the patch is going to be larger. The simulated results for the performance of the antennas are summarized in Table 2.

Finally, in each frequency the radiations patterns of the present designs are also simulated in E-plane ($\varphi = 0°$) and H-plane ($\varphi = 90°$) and plotted in Figures 8(a) & 8(b) and 9(a) & 9(b). From the results obtained, good right-hand CP radiation is observed in all antennas but the difference between RH-CP and LH-CP is improved where in the antenna shown in Figure 3(b) the difference ≈ 2 dB but for the antenna shown in Figure 3(c) the difference ≈ 8 dB. In addition, in both antennas the radiation patterns have maintained their omnidirectional behavior in the upper half plane.

4. CONCLUSION

A new small circular polarized patch antenna suitable for WIMAX and C-band application is proposed. The antenna comprises three N-shaped slots added on the patch to provide the required multi-band as well as reducing the overall antenna size. Some problems rose up due to the small size such as decreasing the impedance bandwidth and relatively low gain. So, the other design has been introduced which has an electromagnetic band gap structure (EBG) to reject the surface waves. Therefore, the efficiency has increased, operational bandwidth improved, and gain gone up.

REFERENCES

1. Gupta, V. R. and N. Gupta, "Characteristics of a compact circularly polarized microstrip antenna," *ISSN Elektronika ir Elektrotechnika*, Vol. 3, No. 52, 1392–1215, 2004.
2. Garg, R., P. Bhartia, I. Bahl, and A. Ittipiboon, *Microstrip Antenna Design*, Artech House, Norwood, MA, 2001.
3. Chen, Y. and C. F. Wang, "Characteristic-mode-based improvement of circularly polarized U-slot and E-shaped patch antennas," *IEEE Antennas and Wireless Propagation Letters*, Vol. 11, 1474–1477, 2012.
4. Shaalan, A. A., "Design and simulation of a single feed dual-band (symmetrical/asymmetrical) U-slot patch antenna," *XLIV International Scientific Conference, Information, Communication and Energy Systems and Technologies (ICEST 2009)*, Veliko Tarnovo, Bulgaria, 2009.
5. Tong, K. F., K. M. Luk, K. F. Lee, and R. Q. Lee, "A broadband U-slot rectangular patch antenna on a microwave substrate," *IEEE Trans. Antennas Propagation*, Vol. 48, 954–960, 2000.
6. Ang, B.-K. and B.-K. Chung, "A wideband E-shaped microstrip patch antenna for 5–6 GHz wireless communications," *Progress In Electromagnetics Research*, Vol. 75, 397–407, 2007.
7. Liu, W. C., "Design of a probe-fed H-shaped microstrip antenna for circular polarization," *Journal of Electromagnetic Waves and Applications*, Vol. 21, No. 7, 857–864, 2007.
8. Rastogi, P. and K. Cecil, "S and C bands multilayer T-slots photonic band gap micro strip antenna," *IOSR Journal of Engineering*, Vol. 2, No. 4, 773–776, 2012.
9. Tlili, B., "Design of C-slot microstrip patch antenna for WiMAX application," *IEEE Trans. Antennas Propagation*, Vol. 16, 521–524, 2009.
10. Jolani, F. and A. M. Dadgarpour, "Compact M-slot folded patch antenna for WLAN," *Progress In Electromagnetics Research Letters*, Vol. 3, 35–42, 2008.

11. Yablonovitch, E., "Photonic band-gap structures," *Journal Optical Society of America*, Vol 10, No. 2, 283–295, 1993.
12. Brown, E. R., C. D. Parker, and E. Yablonovitch, "Radiation properties of a planar antenna on a photonic-crystal substrate," *Journal Optical Society of America*, Vol. 10, No. 2, 404–407, 1993.
13. Sievenpiper, D. F., "High impedance electromagnetic surfaces," Ph.D. Dissertation, Electrical Engineering Department, University of California, Los Angeles, 1999.
14. Yang, F. and Y. Rahmat-Samii, *Electromagnetic Band Gap Structures in Antenna Engineering*, Cambridge University Press, New York, 2008.
15. Guo, S., "Plane wave expansion method for photonic band-gap calculation using matlab," Ph.D. Dissertation, Department of Electrical & Computer Engineering, Old Dominion University, 2001.
16. Meade, R. D., K. D. Brommer, A. M. Rappe, and J. D. Joannopoulos, "Existence of a photonic band gap in two dimensions," *Appl. Phys. Lett.*, Vol 61, 495, 1992.
17. Weily, A. R., K. P. Esselle, B. C. Sanders, and T. S. Bird, "A woodpile EBG sectoral horn antenna," *IEEE Trans. Antennas Propagation*, Vol 51, No. 10, 323–326, 2005.
18. Herbertz, K., "Design and characterization of electromagnetic bandgap filters," Ph.D. Dissertation, Optical and Semiconductor Devices Group, Department of Electrical and Electronic Engineering, Imperial College London, 2010.
19. Barakat, A. and M. El-Khamy, "Bandwidth extension of UWB planar antenna with band-notched characteristics," *IEEE APS, Middle East Conference on Antennas and Propagation (MECAP)*, 1–5, 2010.
20. Ahmed, M. F., A. A. Shaalan, and K. H. Awadalla, "Multi-band novel circularly polarized compact microstrip antenna for applications in modern wireless communications," *The 30th National Radio Science Conference, NRSC 2013*, Vol. 32, 56–63, Egypt, 2013.
21. Munson, R. E., "Conformal microstrip antennas and microstrip phased arrays," *IEEE Trans. Antennas Propagation*, Vol. 22, 74–78, 1974.
22. Ansoft Corporation, *Ansoft High Frequency Structure Simulator v9 User's Guide*, USA, 2013.
23. Computer Simulation Technology Corporation, *CST Licensing Guide 2010*, 2010.
24. Anguera, J., L. Boada, C. Puente, C. Borja, and J. Soler, "Stacked H-shaped microstrip patch antenna," *IEEE Trans. Antennas Propagation*, Vol 52, No. 4, 983–993, April 2004
25. Chaloupka, H., Chaloupka, N. Klein, M. Peiniger, H. Piel, A. Pischke, and G. Splitt, "Miniaturized high-temperature superconductor microstrip patch antenna," *IEEE Trans. Microwave Theory Tech.*, Vol 39, No. 9, 151–1521, 1991.
26. Anguera, J., I. Sanz, J. Mumbú, and C. Puente, "Multi-band handset antenna with a parallel excitation of PIFA and slot radiators," *IEEE Trans. Antennas Propagation*, Vol 58, No. 2, 348–356, Feb. 2010.
27. Anguera, J., A. Andújar, M.C. Huynh, C. Orlenius, C. Picher, and C. Puente, "Advances in antenna technology for wireless handheld devices," *International Journal on Antennas and Propagation*, Vol. 2013, Article ID 838364, 2013.